Blood Stem Cell Activity Is Arrested by Th1-Mediated Injury Preventing Engraftment following Nonmyeloablative Conditioning

Antonia M. S. Müller,*,† Mareike Florek,* Holbrook E. K. Kohrt,‡,1 Natascha J. Küpper,* Alexander Filatenkov,§ Jessica A. Linderman,* Husein Hadeiba,¶ Robert S. Negrin,* and Judith A. Shizuru*

T cells are widely used to promote engraftment of hematopoietic stem cells (HSCs) during an allogeneic hematopoietic cell transplantation. Their role in overcoming barriers to HSC engraftment is thought to be particularly critical when patients receive reduced doses of preparative chemotherapy and/or radiation compared with standard transplantations. In this study, we sought to delineate the effects CD4+ cells on engraftment and blood formation in a model that simulates clinical hematopoietic cell transplantation by transplanting MHC-matched, minor histocompatibility–mismatched grafts composed of purified HSCs, HSCs plus bulk T cells, or HSCs plus T cell subsets into mice conditioned with low-dose irradiation. Grafts containing conventional CD4+ T cells caused marrow inflammation and inhibited HSC engraftment and blood formation. Posttransplantation, the marrows of HSCs plus CD4+ cell recipients contained IL-12–secreting CD11c+ cells and IFN-γ–expressing donor Th1 cells. In this setting, host HSCs arrested at the short-term stem cell stage and remained in the marrow in a quiescent cell cycling state (G0). As a consequence, donor HSCs failed to engraft and hematopoiesis was suppressed. Our data show that Th1 cells included in a hematopoietic allograft can negatively impact HSC activity, blood reconstitution, and engraftment of donor HSCs. This potential negative effect of donor T cells is not considered in clinical transplantation in which bulk T cells are transplanted. Our findings shed new light on the effects of CD4+ T cells on HSC biology and are applicable to other pathogenic states in which immune activation in the bone marrow occurs such as aplastic anemia and certain infectious conditions. *The Journal of Immunology*, 2016, 197: 4151–4162.

T he bone marrow (BM) is a complex microsystem that supports lifelong blood production. BM contains primitive hematopoietic stem cells (HSCs), multipotent progenitors

*Division of Blood and Marrow Transplantation, Department of Medicine, Stanford University School of Medicine, Stanford, CA 94305; †Department of Hematology, University Hospital Zurich, 8091 Zurich, Switzerland; ‡Division of Oncology, Department of Medicine, Stanford University School of Medicine, Stanford, CA 94305; §Division of Immunology and Rheumatology, Department of Medicine, Stanford University School of Medicine, Stanford, CA 94305; and ¶Laboratory of Immunology and Vascular Biology, Department of Pathology, Stanford University School of Medicine, Stanford, CA 94305

1Deceased.

ORCIDs: 0000-0001-6049-3482 (M.F.); 0000-0002-5165-4173 (A.F.); 0000-0002-2491-1365 (H.H.).

Address correspondence and reprint requests to Dr. Antonia M. S. Müller and Dr. Judith A. Shizuru, Division of Blood and Marrow Transplantation, Department of Medicine, Stanford University School of Medicine, 259 West Campus Drive, CCSR, Stanford, CA 94305-5623. E-mail addresses: anmuelle@stanford.edu (A.M.S.M.) and jshizuru@stanford.edu (J.A.S.)

The online version of this article contains supplemental material.

Abbreviations used in this article: BM, bone marrow; CD4conv, conventional CD4+ CD25− T cell; DC, dendritic cell; GVHD, graft-versus-host disease; HCT, hematopoietic cell transplantation; HSC, hematopoietic stem cell; LT-HSC, long-term HSC; MHC I, MHC class I; MHC II, MHC class II; SPCD4depl, CD4+-depleted splenocyte; ST-HSC, short-term HSC; TBI, total body irradiation; WT, wild-type; XRT, x-ray therapy.

(MPPs), committed precursors, and mature blood cells. Within the BM, HSCs interact with nonhematopoietic stromal cells, osteoblasts, and endothelial cells, commonly referred to as their niche (1–3). At steady-state, most HSCs are quiescent (4, 5), but in situations of increased demand, injury of cells, blood loss, and senescence they dynamically respond to generate more blood. An array of signals can trigger this HSC activity, such as cytokines released during infections, and possibly direct sensing of pathogens via TLRs on HSCs (6–11).

Factors also exist that negatively affect proliferation and differentiation of immature blood cells, which manifest clinically as dearth or absence of one or multiple blood lineages and result in BM failure syndromes (12, 13). Although the cellular and molecular mechanisms are incompletely understood, for certain forms of BM failure it is established that T cell–mediated immune reactions negatively affect hematopoiesis (14). Evidence that the BM is a target of T cell immunity comes from aplastic anemia patients who often respond to immunosuppressive therapy (15–18), and from experimental studies that show that mice can develop BM aplasia after transfer of allogeneic lymphocytes (19–21). IFN-γ in particular is implicated in the pathophysiology of these BM failure syndromes (22). In the serum of patients with aplastic anemia who characteristically show a decline in BM HSCs and progenitors, elevated production of both IFN-γ and its transcription factor T-bet have been noted (23–25). The negative effect of IFN-γ on primitive hematopoietic cells is further supported by the finding that exposure of CD34+ cells to IFN-γ can lead to reduced colony formation in human BM cultures, and high levels of IFN-γ can trigger HSC apoptosis (22, 26).

Despite this longstanding knowledge that BM can be vulnerable to T cell–mediated damage, in the setting of an allogeneic

hematopoietic cell transplantation (HCT), T cells are used to improve engraftment and blood cell reconstitution (27). The idea that donor T cells are necessary to secure engraftment developed from clinical studies performed in the 1980s in which BM allografts were depleted of T cells to reduce the complication of graft-versus-host disease (GVHD), but were associated with increased engraftment failures (28–30). In retrospect, these failures may have been caused in part by reduced progenitor numbers, lost as a consequence of graft manipulation, rather than T cell depletion per se, because engraftment problems did not persist in subsequent trials using newer T cell purging methods (31). However, the experiences with graft failure were sufficiently concerning that standard practice to date continues to be transplantation of unmanipulated allografts, replete with donor T cells, and lethal GVHD remains problematic.

Mouse studies segregating bulk T cells into the CD4$^+$ and CD8$^+$ fractions have convincingly shown that CD8$^+$ and not CD4$^+$ cells potently facilitate HSC engraftment in transplantations performed across MHC disparities (32–34). In the standard strain combinations tested, it was difficult to decipher whether CD4$^+$ cells facilitate HSC engraftment because administration of enriched CD4$^+$ cells at doses expected to augment engraftment resulted in acute GVHD, which was more severe than unfractionated T cells containing equivalent numbers of CD4$^+$ cells (32, 33). Assessment of the capacity of CD4$^+$ cells to facilitate engraftment in an MHC class I (MHC I) disparate strain combination in which GVHD would not limit cell dose (B6.C-H-2^{bm1} into B6.Ly-5.1:pep3^b) showed only a weak engraftment facilitating effect (32).

In the last decade the field of HCT has evolved toward the use of less toxic conditioning regimens (reduced intensity, nonmyeloablative), and with these changes engraftment failure has once again emerged as a significant problem (35). These treatments are better tolerated. However, because higher levels of recipient HSCs and immune cells remain after conditioning treatment, graft rejection occurs with greater frequency than with myeloablative conditioning. Donor T cells contained in the graft are believed to be essential to overcome these more formidable barriers (36), yet understanding the effect of T cells on donor cell engraftment and blood formation remains incomplete.

Our prior studies showed that although donor T cells can eradicate host immune cells and thereby shift the balance to higher levels of donor cell chimerism, this increase in donor cells does not equate with better blood production or immune function. Rather, when compared with T cell–depleted grafts, donor CD4$^+$-containing grafts caused delayed recovery of blood formation and poorer T cell function (37, 38). In this study, we examined in detail the effect of donor CD4$^+$ T cells on the BM environment and HSC engraftment and function in mice transplanted with MHC-matched, minor histocompatibility–mismatched grafts and conditioned with low intensity (sublethal) radiation. We show that under these conditions conventional CD4$^+$CD25$^-$ T cells (CD4$_{convs}$) become activated in the BM, and rather than improve engraftment, this population caused engraftment failure of donor HSCs. Posttransplantation recipients of enriched CD4$^+$ cell grafts had high levels of IL-12 and IFN-γ detectable in the BM. In this Th1-cytokine environment, host HSCs were observed at higher than expected proportions in the BM and were arrested with reduced cell cycle activity at the stage of short-term HSC (ST-HSC). The cumulative result was poor blood formation and lack of donor contribution to hematopoiesis. We hypothesize that HSCs respond to certain inflammatory signals by entering a state of dormancy. Such a response of HSCs to environmental conditions induced by CD4$^+$ cell activation represents a novel mechanism underlying the failure of HSCs to engraft and has bearing on understanding the pathophysiology of BM failure states.

Materials and Methods

Mice

AKR/J mice (H2^k; Thy1.1, CD45.2) served as donors for BALB.K hosts (H2^k, Thy1.2, CD45.2). C57BL/6 mice (H2^b, Thy1.1, CD45.1; Thy1.1, GFP$^+$; or IFN-$\gamma^{-/-}$) were donors for BALB.B mice (H2^b, Thy1.2, CD45.2). Congenic experiments used Thy1.1 CD45.2 GFP$^+$ donors for CD45.1 C57BL/6 recipients. HSC donors were 6–10 wk old; recipients were ≥8 wk at transplant. Mice were bred and maintained under pathogen-free conditions at the Stanford University Research Animal Facility or purchased from Jackson Laboratories [AKR/J and IFN-$\gamma^{-/-}$ C57BL/6 (B6.129S7-Ifngtm1Ts/J)]. Animal studies were approved by the Stanford University Administrative Panel on Laboratory Animal Care.

Isolation and transplantation of HSCs and T lymphocytes

Bone marrow was flushed from tibiae and femurs into HBSS/2% FBS, enriched for c-Kit (3C11) cells by magnetic column separation (CD117 MicroBeads, MACS Separation Columns LS; Miltenyi Biotec, Auburn, CA), and KTLS-HSC were purified by FACS sorting. Lineage staining included Abs for CD3ε, CD4, CD5, CD8α, B220, Gr1, Mac1, and Ter119. For cotransfer of T cells, CD4$^+$ and CD8$^+$ cells were extracted from spleens by magnetic column separation to a purity of >90% (CD4/CD8α MicroBeads; Miltenyi Biotec). CD4$^+$CD25$^-$ CD4$_{convs}$ were FACS separated from CD4$^+$-enriched splenic populations.

BALB.K and BALB.B recipients received a sublethal 400 cGy dose of total body gamma irradiation and C57BL/6 recipients received a 475 cGy dose 5 h before tail-vein injection of a radioprotective dose of 3000 KTLS-HSCs. In cotransfer experiments, 1×10^6 CD4$^+$ or CD8$^+$ T cells (CD4$^+$+CD8$^+$ = total T cells) or titrated doses of CD4$^+$CD25$^-$ CD4$_{convs}$ (between 3×10^4 and 3×10^6 for the titration, then 5×10^5 for the remainder of the experiments) were injected simultaneously with the HSCs. In one experiment, recipients were pretreated with two doses of 100 μl of the anti-NK cell polyclonal anti-asialo GM1 Ab before transplant on day −7 i.v. and day −1 i.p. After HCT, mice were monitored for survival, weight loss, and clinical signs of GVHD.

Engraftment and chimerism

Multilineage hematopoietic reconstitution and chimerism were assessed by FACS at 4, 6, and 12 wk post-HCT. Blood lineage phenotypes and chimerism in the C57BL/6 into BALB.B model was done using CD45.1/CD45.2 markers and GFP to distinguish donor-host origin of cells. For the AKR/J into BALB.K model, donor-host T cells were distinguished using Thy1.1$^+$ (donor) and Thy1.2$^+$ (host) markers. Chimerism analysis of B cells, granulocytes, and CD11c$^+$ cells required PCR for D6mit3, a microsatellite marker with informative polymorphism for AKR/J and BALB.K. Genomic DNA was isolated from FACS-sorted populations using the DNeasy Kit according to the manufacturer's instructions (Qiagen, Valencia, CA). Standard PCR conditions were used. PCR amplicons were stained with ethidium bromide for allele determination on 2% agarose gels.

For analysis of BM and spleen cells, extracellular and intracellular stainings were performed according to standard protocols. For measurement of intracellular IFN-γ and IL-17, cells were stimulated with PMA, ionomycin, and monensin; for measurement of IL-12, IL-10, and TNF-α, specimens were incubated with LPS and monensin. Samples were analyzed and sorted on the Stanford Shared FACS facility FACS instruments (LSRII, FACSAria; Becton Dickinson, Mountain View, CA).

Cell harvest, Ab staining, and flow cytometry

BM cells were flushed from the leg bones into staining buffer (2% bovine calf serum/PBS). Spleens were manually processed into single-cell suspensions. RBC lysis was performed with ammonium chloride sodium acetate. Washed cells were blocked with Fcγ-block (10 min) and Abstained for 30 min on ice. For measurement of intracellular IL-17A and IFN-γ expression of lymphocytes, cell suspensions were stimulated with 40 ng/ml PMA (a proteinase kinase C activator), ionomycin (1 μg/ml), and monensin (2 μM; all from Sigma-Aldrich) for 5 h at 37˚C before staining. To assess the IL-12, IL-10, and TNF-α secretion of dendritic cells (DCs), specimens were incubated for 14 h with LPS (5 μg/ml) and monensin before staining. After surface staining, specimens were fixed and permeabilized using a Foxp3 Staining Buffer Set (eBioscience) and Abstained for the intracellular cytokines. For apoptosis studies the Annexin V Apoptosis Detection Kit (eBioscience) with a fixable viability dye (eBioscience) was used and for cell cycle studies the Vybrant DyeCycle stain (Invitrogen) was used according to the manufacturers' instructions. Propidium iodide staining, ethidium monoazide, or a viability kit (LIVE/DEAD Fixable Aqua Dead Cell Stain Kit; Invitrogen) was used to exclude dead cells.

Abs used for FACS were specific for c-Kit (2B8), Thy1.1 (OX-7), Sca-1 (D7), lineage markers CD3ε (145-2C11 or 17A2), CD4 (GK1.5), CD5 (53-7.3), CD8α (53-6.7), B220 (RA3-6B2), Gr1 (RB6-8C5), Mac1 (M1/70), and TER-119 (TER-119), and in addition, anti-CD25 (PC61.5), CD45.1 (A20), CD45.2 (104), CD150 (SLAM) (TC15-12F12,2), CD34 (RAM34), Flt3/CD135 (A2F10), TCR-β (H57-597), Thy1.2 (53-2.1), CD49b (DX5), CD122 (TM-b1), CD11c (N418), CD40 (HM40-3), MHC II (I-A/I-E) (M5/114.15.2), IL-12/IL-23 p40 (C17.8), IFN-γ (XMG1.2), TNF-α (MP6-XT22), and IL-17A (ebio17B7). Abs were from eBioscience, Biolegend, Invitrogen, or BD Biosciences. Samples were analyzed and sorted on the Stanford Shared FACS facility Hi-Dimensional FACS instruments (LSRII, FACSAria).

Histopathology

Femurs were fixed in 10% neutralized formalin (24 h), decalcified in 0.375 M EDTA (12 d), and paraffin embedded. Embedding and H&E staining were performed by the Histo-Tec Laboratory (Hayward, CA). Pictures were taken on a Leica CTR 5000 digital microscope with a Leica FDC 425 camera.

Statistical methods

Microsoft Excel software was used to create weight curves and to assess p values for groups by two-tailed Student t test. GraphPad Prism 4.0 software was used to create Kaplan–Meier survival curves, and column-bar diagrams, displaying the mean and SEM, were created using GraphPad Prism 4.0 software.

Results

Donor CD4+ cells impair donor and host hematopoiesis after sublethal irradiation

We used a model of sublethal irradiation and transplantation of MHC-matched, minor Ag–mismatched hematopoietic cells, which approximates clinical nonmyeloablative HCT regimens. BALB.K ($H2^k$) recipients were treated with 400 cGy of total body irradiation (TBI) and infused with AKR/J ($H2^K$) grafts. Grafts contained 3000 FACS-purified KTLS-HSCs, or HSCs plus unfractionated splenic T cells or 1×10^6 selected CD4+ or CD8+ T cells. All recipients survived and only transient weight loss was observed, which was most pronounced in HSC+CD4+ cell recipients, and these animals recovered by 3 wk posttransplant (Fig. 1A). Except for this transient weight loss, no evidence of overt GVHD was observed.

Despite recovery and survival of all transplanted mice, recipients of grafts that contained CD4+ cells had marked cytopenias early posttransplant and delayed lymphocyte reconstitution compared with recipients of HSCs alone or HSC+CD8+ cells. Fig. 1B shows the absolute cell numbers in the BM and spleens of recipients on day +14 post-HCT. Total cellularity was significantly reduced in HSC+CD4+ cell recipients compared with all other groups and was even worse than in untransplanted radiation x-ray therapy (XRT) controls. Histologic evaluation of BM from femurs at sequential time points early posttransplant confirmed profound hypocellularity in HSC+CD4+ recipients at day +14, which contrasted the robust hematopoietic regeneration observed in recipients of HSC only beginning as early as day +10 (Fig. 1C). Analysis at day +28 of the blood of mice given grafts containing CD4+ T cells was notable for marked lymphopenia, which upon closer examination preferentially affected B cells (Fig. 1D, 1E, Supplemental Fig. 1A). Granulocytes, CD4+ T cells, and CD8+ T cells were also reduced in number compared with unmanipulated mice, but differences between groups were not as pronounced as for the B lineage (Supplemental Fig. 1A).

In addition to the cytopenias precipitated by donor CD4+ cells, CD4+ T cells in the donor inoculum impaired donor cell engraftment. Determination of the origins of blood production in recipients at 6 wk and beyond (>14 wk) showed that most mice given CD4+ cell–containing grafts did not generate B or T cells from the donor source, and the donor graft produced only low levels of myeloid cells (detectable by PCR). In contrast, mice

transplanted with HSCs alone or HSC+CD8+ cells showed mixed chimerism in all lineages (Fig. 1F–H, Supplemental Fig. 1B).

We confirmed that the observed negative effects of donor CD4+ T cells on blood cell production were not strain specific by performing identical studies across a different MHC-matched allogeneic strain combination [C57BL/6 into BALB.B ($H2^b$)]. HSC+CD4+ recipients displayed the same pattern of lymphopenia and poor donor cell engraftment in all blood lineages. Again, contrasting the hematopoietic recovery of HSC+CD4+ cell recipients, mice that received HSC or HSC+CD8+ cells demonstrated robust and long-lasting production of both donor- and host-derived cells (mixed chimerism) of all blood lineages (Supplemental Fig. 1C).

Segregation of the coinfused CD4+ T cells into $CD4_{conv}$ and regulatory (CD4+CD25+) subsets revealed that the BM-suppressive activity was confined to the $CD4_{conv}$ population, which impaired lymphocyte reconstitution at relatively low doses. In fact, the effect of $CD4_{convs}$ was more deleterious than unselected CD4+ T cells because even low doses of $CD4_{convs}$ were able to cause lethal GVHD (Supplemental Fig. 2A–C).

These negative effects of donor CD4+ T cells occurred only in allogeneic and not in congenic strain pairs, indicating alloantigen recognition by CD4+ cells drives this process leading to B cell and other cytopenias (Supplemental Fig. 2D–F).

Th1-type skewing of immune cells in the BM

To characterize the suppressive environment induced by infusion of $CD4_{convs}$, we analyzed BM and spleens of BALB.K recipients of AKR/J HSC+$CD4_{conv}$ for cellularity, lineage types, and cytokine activity. Results were compared with those obtained from recipients of HSCs, HSC+CD8+-enriched cell recipients (CD4+-depleted splenocytes [$SP_{CD4depl}$] or positively selected CD8+ splenocytes), XRT controls, and unmanipulated wild-type (WT) animals. At day 14 post-HCT, BM from these latter groups had low T cell levels, whereas HSC+$CD4_{conv}$ recipients demonstrated a marked proportional (but not absolute) increase of CD4+ T cells (Fig. 2A, Supplemental Fig. 1A). CD4+ T cells in HSC+$CD4_{conv}$ recipients were of mixed chimerism with a donor/host ratio significantly higher in BM compared with spleens (Fig. 2B).

Intracellular staining and FACS analyses were performed to examine the BM cytokine milieu of transplant recipients. Because baseline cytokine levels are typically low to undetectable in BM T cells, samples were stimulated with PMA before analysis. Fig. 2C and 2D show that at day 14 post-HCT the highest levels of IFN-γ–secreting cells within the CD4+ T cell population were present in the BM of HSC+$CD4_{conv}$ recipients. This proportion was significantly higher in the BM than in the spleen of these recipients ($p = 0.001$). Costaining with Thy1.1 identified donor cells as the main source of IFN-γ (Fig. 2C, 2D). Taken together, these data suggest that donor T cells not only reach the BM by distribution with the blood circulation, but that the BM is a sensitive target of donor CD4+ T cells that, upon encounter with alloantigen, expand and mount a Th1-biased immune response with prominent production of IFN-γ.

The polarized IFN-γ response was transient, and by day 28 post-HCT IFN-γ expression had returned to baseline in all groups. Expression of IL-10 and IL-17 by BM or spleen cells was not observed in any of the treatment groups, neither at day 14 nor at day 28 post-HCT.

The BM of HSC+$CD4_{conv}$ recipients contained significantly higher proportions (but not absolute numbers) of NK cells compared with other groups. Administration of the NK cell–depleting polyclonal anti-asialo GM Ab before HCT improved T cell recovery somewhat, but this increase of donor T cells did not reach statistical significance, suggesting that NK cells are not key mediators in suppressing donor cell development (Supplemental Fig. 3A–D).
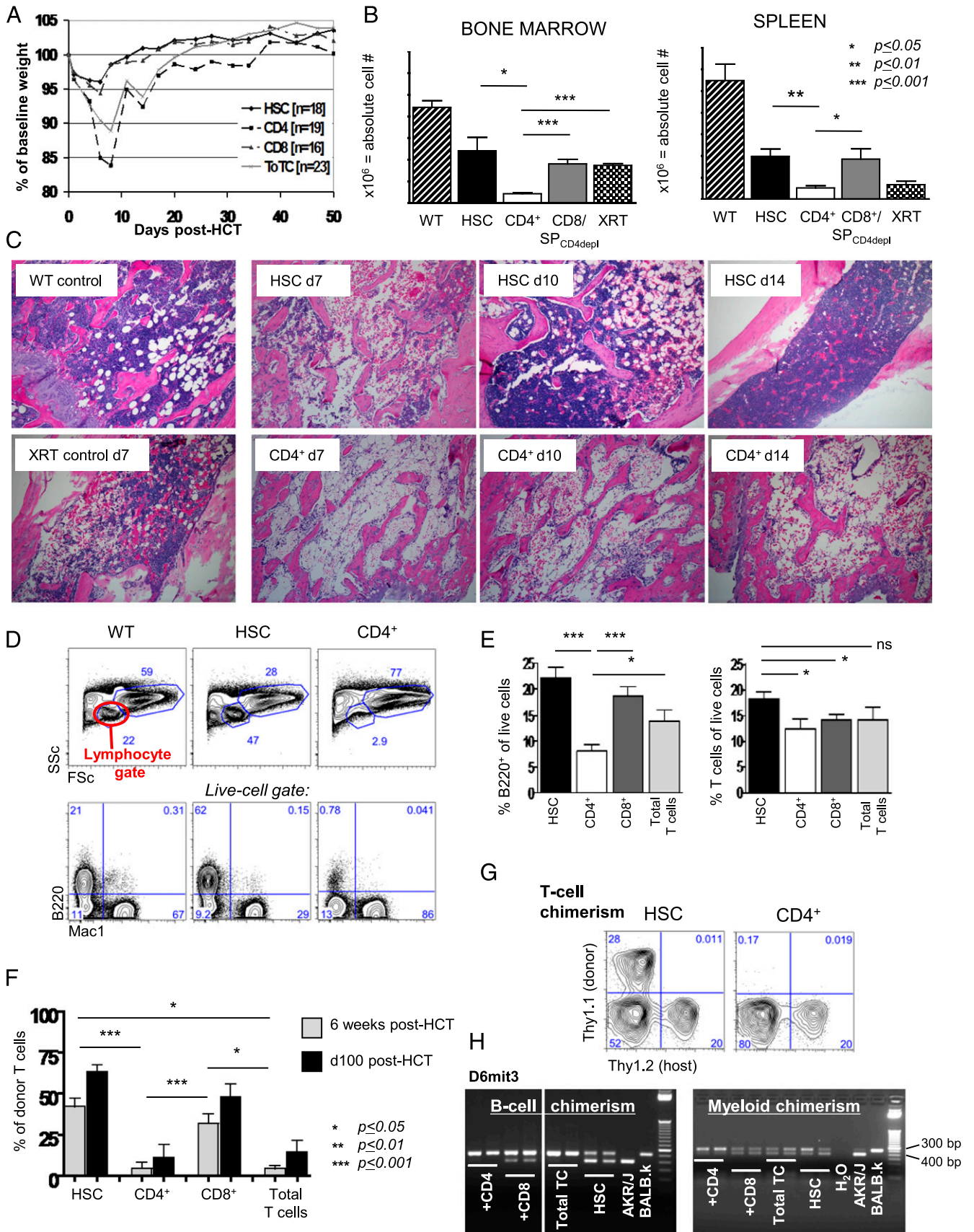
FIGURE 1. Donor CD4^{+} T cells cause BM aplasia and engraftment failure. Experimental schema: BALB.K (H2[k]) or BALB.B (H2[b]) mice underwent sublethal 400 cGy TBI and were infused with 3000 AKR/J (H2[k]) or C57BL/6 (H2[b]) KTLS-HSC (c-Kit^{+}Thy1.1^{lo}Lin^{neg}Sca-1^{+}), respectively. HSCs were given alone or in combination with CD4^{+}, CD8^{+}, or CD4^{+}+CD8^{+} (total) T cells. (**A**) Weight course of BALB.K mice that underwent 400 cGy TBI and were infused with 3000 AKR/J HSCs ($n = 16$), HSC+CD4^{+} ($n = 19$), or HSC+CD8^{+} ($n = 19$), or HSC+total T cells ($n = 23$). The weight curves (showing % of baseline weight) indicate a marked weight loss but rapid and complete recovery in mice given HSC+CD4^{+} or HSC+total T cell *(Figure legend continues)*
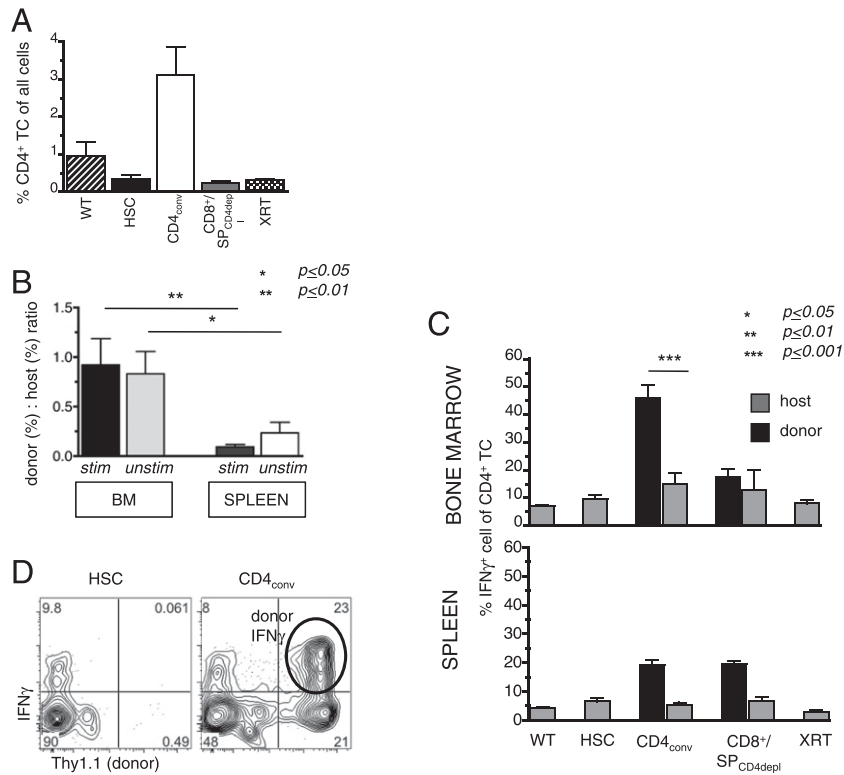
FIGURE 2. Donor CD4^{+} T cells induce Th1 immune reactions in the marrow post-HCT. As in Fig. 1A, BALB.K mice were transplanted with AKR/J (both H2[k]) KTLS-HSCs alone or in combination with CD4$_{conv}$ T cells (CD4^{+}CD25^{−}), or CD8^{+}/SP$_{CD4depl}$ (both groups were compiled as one group). BM and spleens of recipients were harvested on day 14 for measurement of cell content and intracellular cytokines. (**A**) BM cells contained higher proportions of CD4^{+} T cells in HSC+CD4$_{conv}$ recipients ($n = 7$) compared with the other groups (WT: $n = 2$; HSC alone: $n = 6$; SP$_{CD4depl}$: $n = 4$; XRT only: $n = 4$), as determined by FACS. (**B**) The ratio of donor to host contribution within the CD4^{+} T cells was calculated by % donor CD4^{+}/% host CD4^{+} T cells of all live cells. In HSC+CD4$_{conv}$ recipients, donor-host ratios were significantly higher in the BM as compared with the spleen for both PMA-stimulated and unstimulated T cells ($n = 11$). (**C**) Compiled data of % IFN-γ^{+} cells of all BM and spleen CD4^{+} T cells (after 6-h PMA stimulation) in WT controls ($n = 2$), recipients of HSC only ($n = 6$), HSC+CD4$_{conv}$ ($n = 7$), HSC+CD8^{+}/SP$_{CD4depl}$ ($n = 4$), or XRT controls ($n = 4$). Percentages of donor- and host-derived IFN-γ^{+} are shown for transplanted groups. (**D**) Representative FACS plots gated on BM CD4^{+} T cells in recipients of HSCs and HSC+CD4$_{conv}$ show intracellular IFN-γ^{+} expression of donor (Thy1.1^{+}) and host (Thy1.1^{−}) CD4^{+} T cells. *$p \leq 0.05$, **$p \leq 0.01$, ***$p \leq 0.001$.

CD11c^{+} cells are increased and activated in the marrow of CD4^{+} T cell recipients

On day 7 post-HCT, HSC recipients, HSC+CD4$_{conv}$ recipients, and XRT controls all had, compared with WT mice, increased percentages of CD11c^{+} cells in their BM that coexpressed MHC II^{+} and CD8^{+} (Fig. 3A). Although proportionally increased, absolute numbers of the total CD11c^{+} cells were reduced in BM and spleen compared with unmanipulated WT controls (Fig. 3B), which was consistent with the low cellularity in these tissues early post-XRT and HCT. Of note, only in the group that received HSC+CD4$_{conv}$ was a subset of CD11c^{+} cells observed to coexpress the activation marker CD40 (Fig. 3C), suggesting that the BM of these mice contained increased proportions of activated DCs compared with all other groups.

Cytokine studies of BM CD11c^{+} cells corroborated the phenotype analyses: measurement of intracellular IL-12, IL-10, and TNF-α expression after LPS stimulation at day 7 post-HCT showed that all groups had elevated secretion of IL-12 compared with WT mice. However, once again, the activity of BM-CD11c^{+} cells from the HSC+CD4$_{conv}$ group was significantly higher compared with HSC or HSC+CD8^{+} recipients, WT, and XRT controls (Fig. 4A–D). Furthermore, only BM-CD11c^{+} cells from HSC+CD4$_{conv}$ recipients expressed persistently high levels of IL-12 at day 14 (Fig. 4D), whereas in all other groups CD11c^{+} cell expansion and IL-12 secretion had returned to baseline. In HSC+CD4$_{conv}$ recipients an IL-12 response was detectable even without LPS stimulation, supporting the occurrence of true in vivo activation of CD11c^{+} cells in these mice (Fig. 4E). This IL-12

grafts. Recipients of HSCs alone or HSC+CD8^{+} had only minimal weight loss and recovered promptly. (**B**) Absolute cell counts from day 14 show significantly reduced cellularity in BM (left) and spleen (right) in recipients of HSC+CD4^{+} ($n = 11$) compared with recipients of HSCs alone ($n = 8$), HSC+CD8^{+} or HSC+CD4-depleted (CD4[depl]) splenocytes ($n = 6$) or XRT controls ($n = 6$). (**C**) H&E staining of long bones of representative transplanted animals on days 7, 10, and 14 post-HCT, an XRT control on day 7, and a WT animal are shown. Original magnification ×10. (**D**) FACS analysis of blood at day 28 post-HCT showed marked reduction of cells in the lymphocyte gate in HSC+CD4^{+} recipients (side scatter [SSC] low/forward scatter [FSC] low, top panel). This lymphopenia resulted primarily from a marked reduction of B cells (lower panel of FACS plots). (**E**) Compiled bar graphs displaying proportions of B220^{+} B cells and T cells of all live cells at 4 wk post-HCT. (**F**) Compiled FACS results displaying donor T cell (Thy1.1) contribution to all live cells at 6 wk (d42) and day +100 post-HCT showing the lowest donor T cell contribution in recipients of CD4^{+} T cell–containing grafts. (**G**) Representative d42 FACS plots of blood measuring Thy1.1^{+} donor versus Thy1.2^{+} host T cells of HSC and HSC+CD4^{+} recipients. (**H**) d42 blood B cell (sorted for B220^{+} cells) and myeloid (sorted for Mac1^{+} cells) chimerism assessed by PCR for D6mit3 revealed absence of donor B cells in HSC+CD4^{+} or HSC+total T cell recipients, and mixed donor-host B cell chimerism in recipients of HSC alone or with CD8^{+}. In contrast, myeloid cells were of mixed chimerism in all groups. Two representative examples per group are shown. *$p \leq 0.05$, **$p \leq 0.01$, ***$p \leq 0.001$.
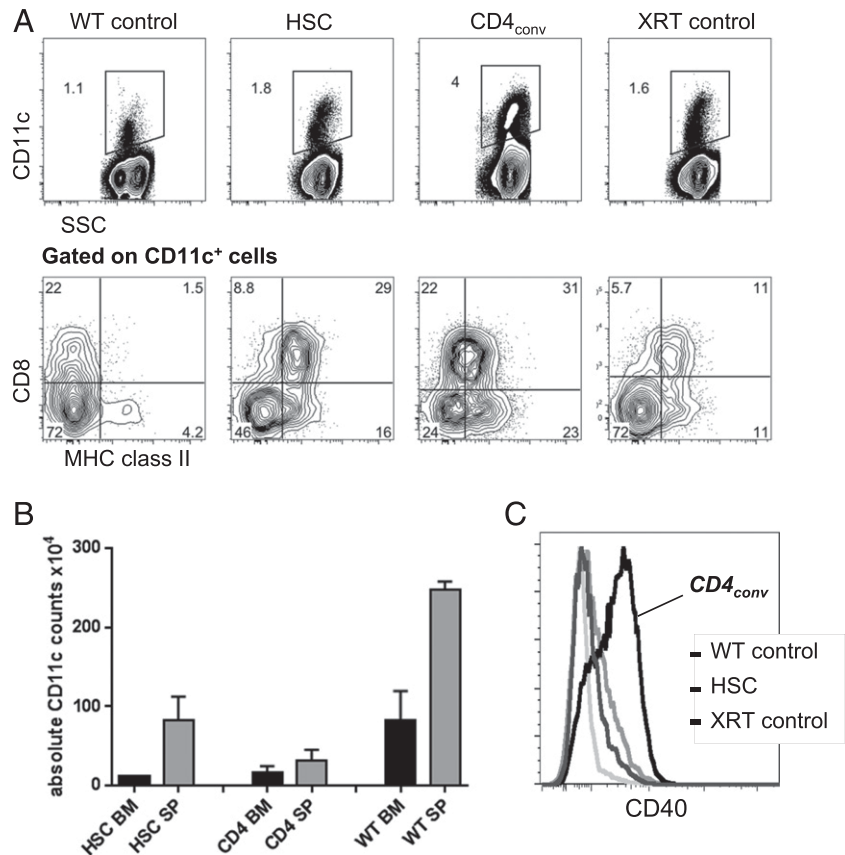
FIGURE 3. Higher levels of activated CD11c+ cells are found in the marrow of CD4+ T cell recipients. (**A**) Representative FACS plots show the proportion of CD11c+ cells of all live cells in the BM of WT mice, recipients of HSCs, recipients of HSC+CD4$_{conv}$, and XRT controls on day 7 post-HCT (upper panels) and their coexpression of CD8+ and MHC II (lower panels, gated on CD11c+). (**B**) Absolute counts of CD11c+ cells in the BM (black bars) and spleen (gray bars) of sublethally irradiated BALB.K recipients of AKR/J HSCs or HSC+CD4+ at 2 wk post-HCT as compared with WT controls, showing no significant differences in absolute cell counts in both experimental groups, but higher numbers in the WT mice. (**C**) Representative FACS histograms showing CD11c+ cells had increased CD40 expression in HSC+CD4$_{conv}$ recipients compared with controls at 1 wk post-HCT.

response was limited to the BM (with or without LPS stimulation), whereas splenic levels were low (Fig. 4F). There was no detectable IL-10 production or TNF-α increases in any of the groups. We conclude that early post-HCT HSC+CD4$_{conv}$ recipients develop a unique BM environment containing activated CD11c+ DCs that played a role in driving the Th1-biased response.

CD4+ T cell–mediated inflammation prevents proliferation and maturation of HSCs

To this point our data suggested the Th1-skewed inflammatory marrow environment suppresses hematopoiesis and, as a consequence, impairs donor HSC engraftment. To further examine the stem and progenitor cell pool, we harvested BM at day 14 post-HCT for FACS analysis. Fig. 5A shows that, in WT BALB.K mice, the lin^{neg} IL-7Rα^{neg} fraction contains c-Kit$^+$Sca-1$^-$ myeloid progenitors and c-Kit$^+$Sca-1$^+$ KLS-HSCs. KLS-HSCs can be further subdivided into CD34$^+$Flt3$^+$ MPPs and CD34$^-$Flt3$^-$ true-HSC (long-term HSC [LT-HSC] and ST-HSC) (Fig. 5A, upper panels). In recipients of HSC alone, the KLS-HSC pool was composed of both MPPs and HSCs, and resembled the subset distribution of WT animals (Fig. 5A, middle panels, 5B). In contrast, HSC+CD4$_{conv}$ recipients had an abnormally large population of KLS-HSCs, of which only a small proportion were MPPs (Fig. 5A, lower panels, 5B). Within the true-HSC compartment, LT-HSCs can be distinguished from ST-HSCs by SLAM (CD150) expression. Using this phenotypic discrimination in HSC+CD4$_{conv}$ recipients, there was a marked shift from LT-HSCs to ST-HSCs compared with WT mice (Fig. 5C).

The atypical predominance of true LT-HSCs and ST-HSCs, but lack of MPPs, in the BM of HSC+CD4$_{conv}$ recipients led us to assess their proliferative status and cell cycle activity. At day 7 post-HCT in HSC+CD4$_{conv}$ recipients, the majority of KLS-HSCs and myeloid progenitors were in the G$_{0/1}$ resting stage. The quiescent status of

myeloid progenitors contrasted the increased S-synthesis cell cycle activity observed in pure HSC recipients (Fig. 5D).

Apoptosis of donor progenitors is not the cause of engraftment failure

To examine the fate of donor progenitors and whether their cell death was triggered by the Th1 proinflammatory microenvironment, we measured apoptosis in BM and spleen. Surface marker and Annexin V staining on day 11 post-HCT revealed high levels of apoptosis in the mature lineage cells of the host, which had been exposed to irradiation. Apoptosis in the c-Kit$^+$ progenitor fractions affected host progenitor cells more than donors and was higher in HSC+CD4$_{conv}$ recipients compared with HSC recipients (Supplemental Fig. 3E, 3F). At the same time these findings suggest that the poor donor engraftment in HSC+CD4$_{conv}$ recipients was not due to apoptosis of donor-derived progenitors.

HSCs remain functional in response to CD4-mediated immune injury

To test the functional competence of the enlarged ST-HSC and LT-HSC population present in the Th1-skewed BM environment of HSC+CD4$_{conv}$ recipients, we performed adoptive transfer studies into secondary recipients. KTLS-HSC+CD4$_{conv}$ from AKR/J primary (first) donors were transplanted into sublethally irradiated BALB.K first recipients (both H2^k). At day 14 post-HCT, KLS-CD34$^-$Flt3$^-$SLAM$^+$ (LT-HSCs) and SLAM$^-$ (ST-HSCs) were FACS-purified and infused into sublethally irradiated Rag2γc$^{-/-}$ C57BL/6 secondary (second) recipients (H2^b) that lack lymphoid cells (Fig. 6A), and thus have no immune barrier to actively reject MHC-mismatched grafts. Chimerism analyses at 1 and 3 mo post-HCT revealed that the H2^{k+} ST-HSCs and LT-HSCs from the first recipients conferred sustained hematopoiesis of all lineages in second recipients. T cell lineage analysis revealed that only
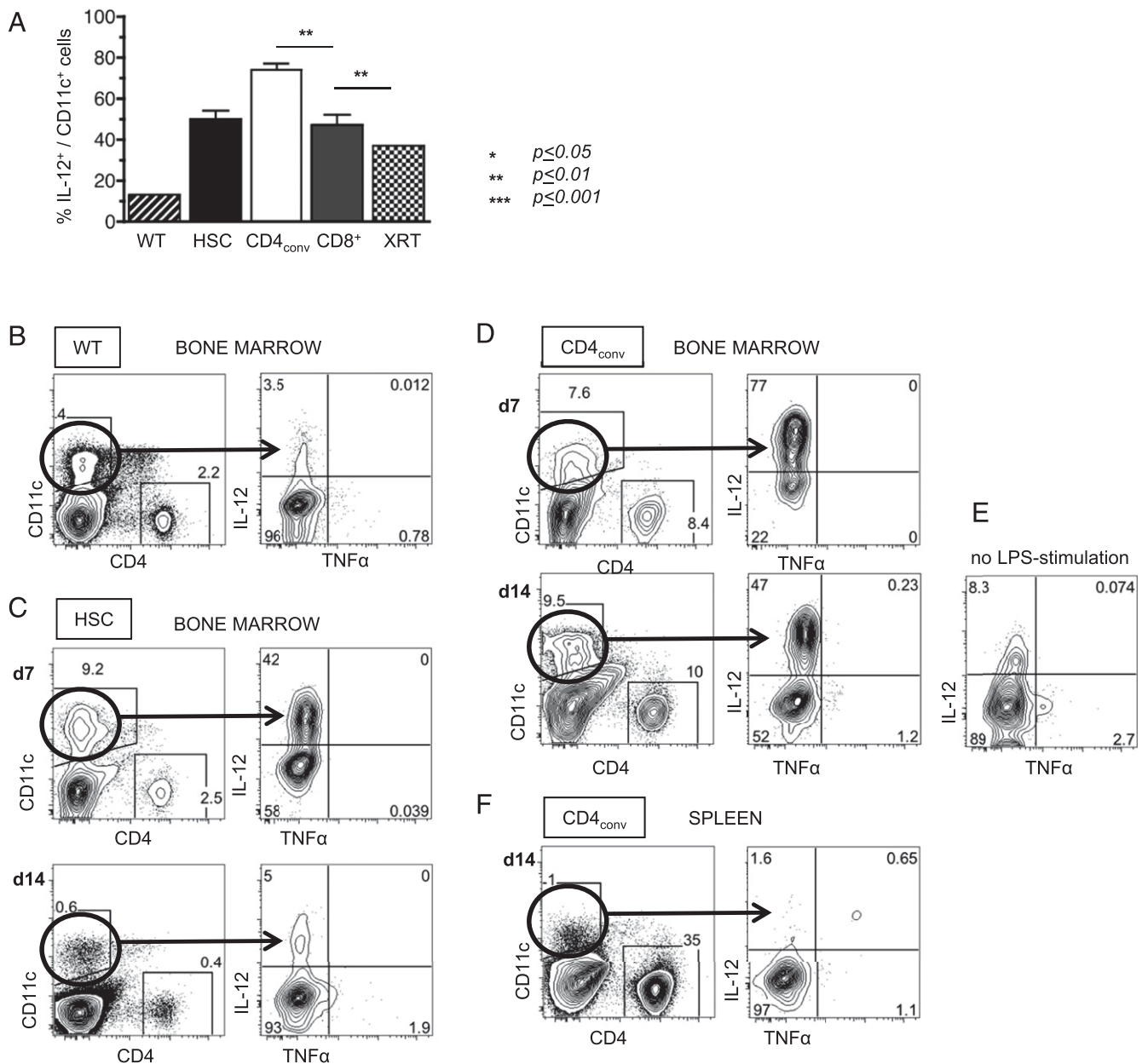
FIGURE 4. IL-12–secreting CD11c^{+} DCs persist in recipients of HSC+CD4^{+} T cells. (**A**) Compiled data on IL-12 expression of CD11c^{+} DCs in LPS-stimulated BM at day (d) 7 post-HCT showing significantly higher levels of IL-12 in HSC+CD4$_{conv}$ recipients as compared with recipients of HSCs or HSC+CD8^{+} T cells. (**B–F**) Representative FACS plots of WT BM cells (B); BM from HSC recipients on d7 and d14 post-HCT (C); BM from HSC+CD4$_{conv}$ recipients on d7 and d14 post-HCT (D) including an unstimulated control from the same animal (E); spleen from HSC+CD4$_{conv}$ recipients on d14 post-HCT (F) after 14-h in vitro LPS stimulation, displaying CD11c^{+} DCs and their baseline IL-12 expression. (C) In HSC recipients, DCs expanded upon LPS stimulation and expressed IL-12 on d7 post-HCT but normalized by d14. (D) In recipients of HSC+CD4$_{conv}$, DC expansion and IL-12 expression persisted through d14 post-HCT. (E) In recipients of HSC+CD4$_{conv}$, IL-12 expression was also detectable without LPS stimulation. (F) In recipients of HSC+CD4$_{conv}$, no increased IL-12 expression was detectable in the spleen. The number of experimental animals was $n = 3–5$ per time point per group. **$*p \leq 0.01$.

Thy1.2[+] and not Thy1.1^{+} T cells were present, indicating that the developing T cells originated from the first recipient (BALB.K, Thy1.2), and not from the first donor (AKR/J, Thy1.1) (Fig. 6B). However, despite sustained long-term hematopoiesis in the second recipients, levels of donor B and T cell engraftment achieved were significantly lower compared with levels achieved after transplantation of healthy WT KLS-CD34^{−}Flt3^{−}SLAM^{+/−}-HSCs (Fig. 6C). Together, these findings show that within the Th1-inflamed BM of HSC+CD4$_{conv}$ recipients, a viable and quiescent HSC pool was preserved that was: 1) capable of sustained and rapid blood production once removed from the inflamed envi-

ronment, 2) derived entirely from the first recipient (not the first donor), and 3) yet had impaired function as compared with WT-HSCs.

IFN-γ mediates CD4^{+}-induced immune injury and skewing of HSC phenotypes

To further characterize the effect of the Th1-skewed environment on hematopoietic progenitors, we interrogated whether the lack of MPPs and phenotypic arrest of immature cells at the level of ST-HSC was due to increased IFN-γ levels. Thus, CD4$_{convs}$ from either IFN-γ^{−/−} or WT C57BL/6 mice were cotransplanted with
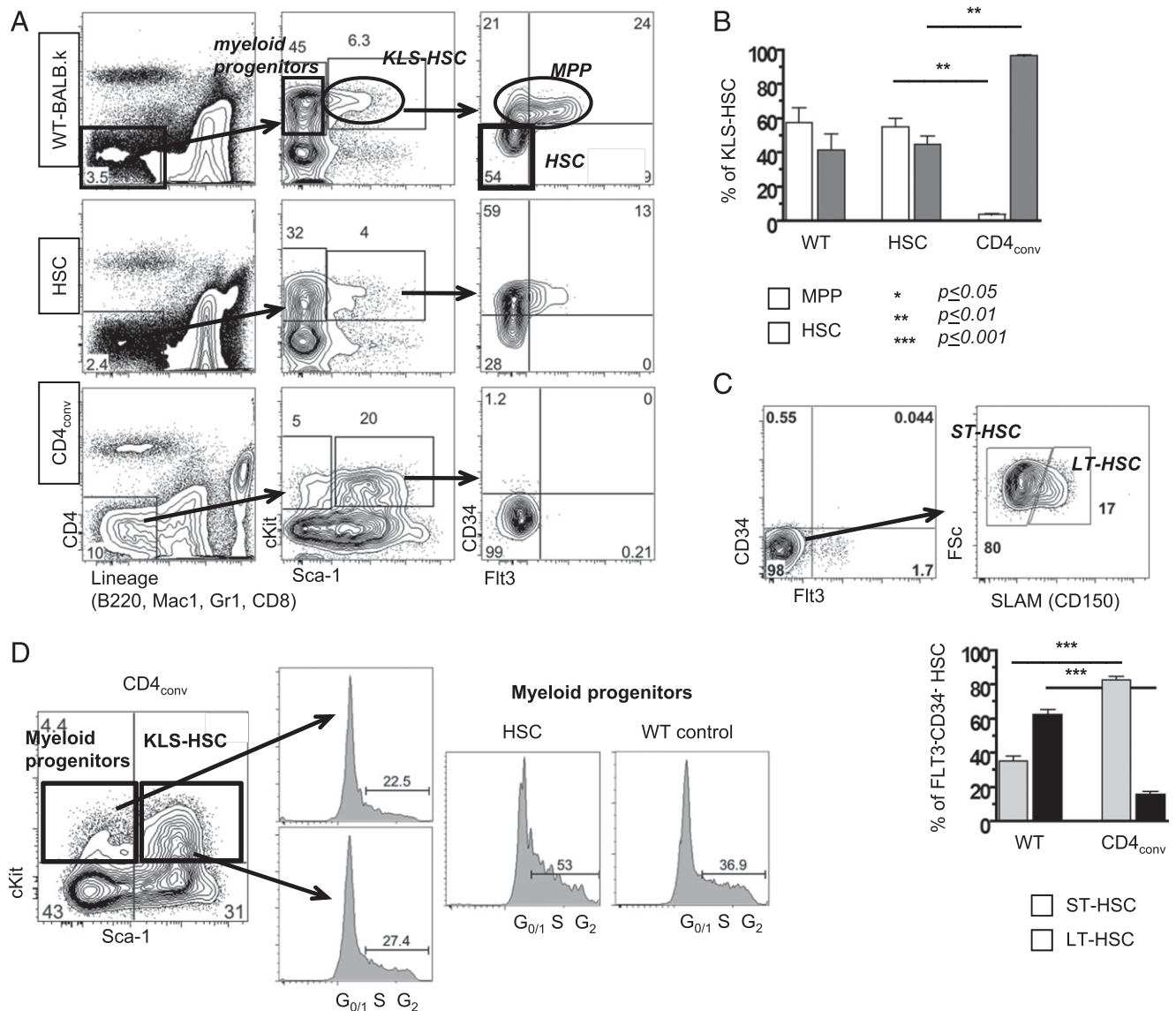
FIGURE 5. CD4$^+$ T cell–mediated inflammation prevents HSC proliferation and maturation. (**A**) Gating schema used to delineate HSC and progenitor subsets. Shown are representative FACS plots for KLS-HSCs and MPPs for WT (top panels), HSC recipients (middle panels), and HSC+CD4$_{conv}$ recipients at day 14 post-HCT. Myeloid progenitors: c-Kit$^+$Sca-1$^-$; KLS-HSC: c-Kit$^+$Sca-1$^+$ which comprise MPPs (CD34$^+$Flt3$^{+/-}$) and true-HSC (CD34$^-$Flt3$^-$). HSC recipients showed normal proportions of myeloid progenitor cells and KLS-HSCs, with increase of MPPs (middle panels). HSC+CD4$_{conv}$ recipients had decreased myeloid progenitor cells but increased proportions of KLS-HSCs (mostly CD34$^-$Flt3$^-$; bottom panels). (**B**) Compiled data of % MPPs and HSCs within KLS-HSCs of WT mice ($n = 5$), HSC recipients ($n = 4$), and HSC+CD4$_{conv}$ recipients ($n = 9$). (**C**) Top panels are representative FACS-HSC staining in the BM of a HSC+CD4$^+$ recipient displaying the gating schema to delineate SLAM$^+$ LT-HSCs and SLAM$^-$ ST-HSCs within the KLS-Flt3$^-$CD34$^-$ HSC compartment. Bottom panel represents compiled data on proportions of LT-HSCs and ST-HSCs within the KLS-Flt3$^-$CD34$^-$ HSC compartment in HSC+CD4$_{conv}$ recipients ($n = 5$) and WT mice ($n = 4$). (**D**) FACS cell cycle analysis of myeloid progenitors and KLS-HSCs was performed with G$_{0/1}$ indicating resting stage, and S and G$_2$ indicating synthesis phase. On day 7 post-HCT, Lin^{neg}-gated BM cells of HSC+CD4$^+$ recipients had decreased myeloid progenitors and increased KLS-HSCs compared with WT control and HSC recipients, and myeloid progenitor cells in HSC recipients and WT mice had a greater proportion of cells in the S-synthesis phase. Shown are FACS plots of representative animals with groups of $n = 2$–4 animals per group. **$p \leq 0.01$, ***$p \leq 0.001$.

WT C57BL/6 HSCs into sublethally irradiated BALB.B recipients. Strikingly, only recipients of HSC+WT CD4$_{conv}$ grafts had an abnormally expanded KLS-HSC population with upregulated Sca-1 expression, whereas mice given HSC+IFN-$\gamma^{-/-}$ CD4$_{conv}$ or control congenic C57BL/6 recipients of HSC+WT CD4$_{conv}$ grafts had a frequency and KLS phenotype identical with unmanipulated WT mice (Fig. 7A). Furthermore, within the expanded KLS-HSC compartment of allogeneic BALB.B recipients given WT CD4$_{conv}$-containing grafts, there was a marked predominance of ST-HSCs and a relative lack of MPPs. In contrast, in allogeneic recipients of HSC+IFN-$\gamma^{-/-}$ CD4$_{conv}$ or congenic recipients of HSC+WT CD4$_{conv}$ grafts, donor MPPs dominated the KLS

population, similar to what is observed in HSC recipients and WT controls (Fig. 7B). Thus, allogeneic CD4$_{convs}$ appear to mediate their effects on the arrest of cell cycling and retention of HSCs in the niche via IFN-γ.

Discussion

Preservation of blood formation requires that BM cells respond dynamically to stress. Although immune cells present in the marrow defend the integrity of this environment, many studies point to the deleterious effects of BM T cell activation on hematopoiesis (14, 19–21, 25). In fact, preclinical models of immune-induced aplasia rely on the high sensitivity of BM to
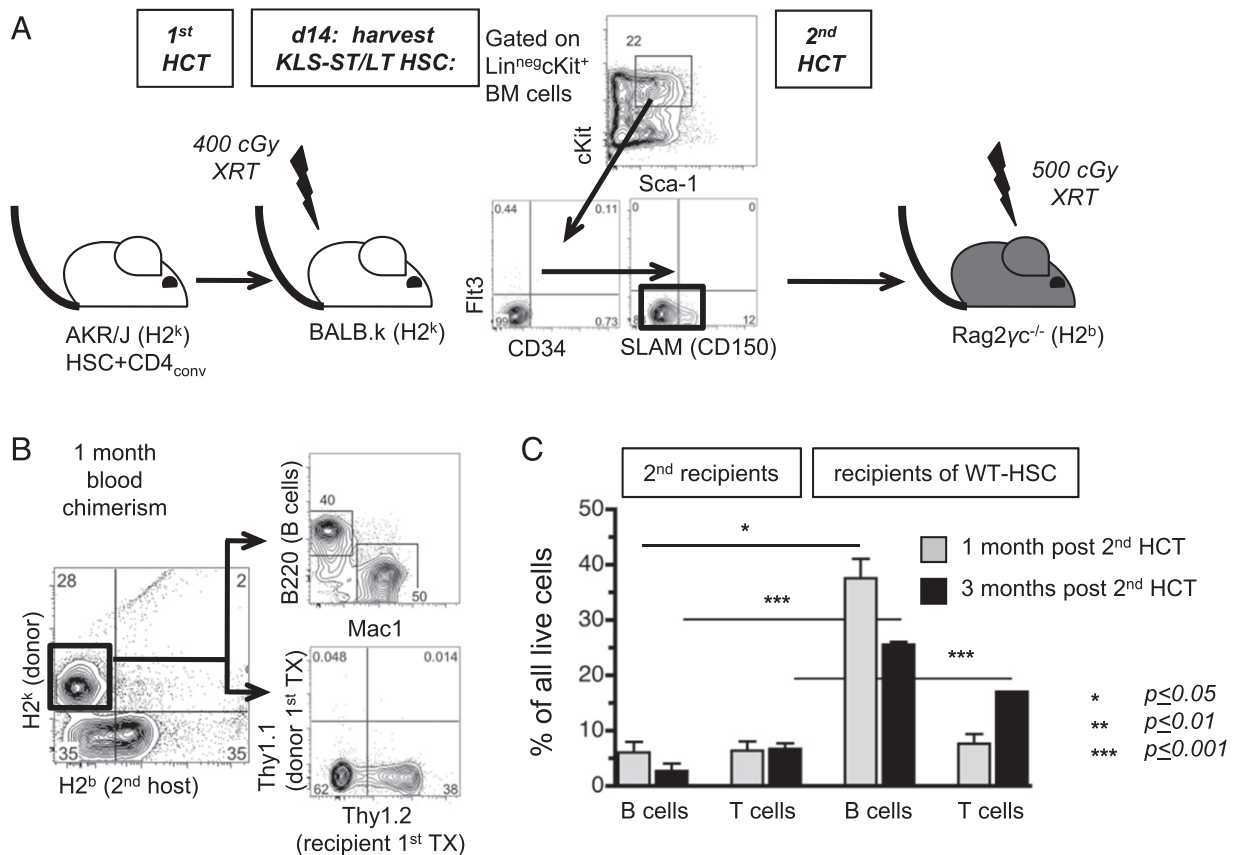
FIGURE 6. Arrested HSCs are viable and retain their potential to sustain hematopoiesis. (**A**) Schema of secondary HCT experiment: BALB.K mice (H2^k; primary [first] recipient) received AKR/J HSC+CD4$_{conv}$ grafts (H2^k; primary donor). On day 14 (d14) post-HCT, BM was harvested from first recipients for FACS isolation of KLS-CD34$^-$Flt3$^-$-HSC. A total of 3500–14,000 cells per mouse was obtained and infused into secondary (second) Rag2γc$^{-/-}$ recipients (H2^b) (each first recipient served as a donor for one second recipient; $n = 5$ first and second recipients, respectively). (**B**) Blood chimerism for B220$^+$, Mac1$^+$, and Thy1$^+$ populations at 1 mo after secondary HCT confirmed H2^{k+} donor cell contribution. No T cells were derived from the first donor (Thy1.1$^+$ AKR/J). (**C**) Compiled data on the level of lymphoid engraftment at 1 and 3 mo post-HCT in Rag2γc$^{-/-}$ recipients of KLS-CD34$^-$Flt3$^-$-HSC grafts derived from first recipients ($n = 5$) as compared with WT donors ($n = 2$). The proportion of B and T cells achieved in second recipients at 1 and 3 mo post-HCT was significantly lower for HSCs that had been exposed to inflammation in the first recipient as compared with 7500 KLS-CD34$^-$Flt3$^-$HSCs derived from WT mice. *$p \leq 0.05$, ***$p \leq 0.001$.

injury by genetically different T cells that become activated by alloantigens. Therefore, in the setting of clinical allogeneic HCT, it is paradoxical that donor T cells are thought to uniformly augment donor HSC engraftment and hematopoiesis (27–30). The newer approaches to BM transplantation using regimens of reduced intensity and the re-emergence of engraftment failure as a problem prompted us to examine the dynamics that occur within the BM after nonmyeloablative, sublethal irradiation and infusion of HSC grafts with or without T cell (subset) supplementation. Rather than eliminate host HSCs and facilitate donor cell engraftment as might be expected, addition of donor CD4$^+$ T cells resulted in the transient suppression but long-term preservation of host hematopoiesis, and at the same time caused failure of donor HSCs to engraft.

Segregation of transferred T cells into subsets revealed that in the context of sublethal irradiation, donor CD4$^+$ T cells substantially altered the BM environment of the recipients. Conventional donor CD4$^+$CD25$^-$ T cells initiated a chain of immunogenic events with Th1-skewed reactivity that caused marrow aplasia with subsequent slow recovery of blood formation. Even low numbers of donor CD4$^+$ T cells induced BM hypocellularity, despite animals otherwise showing no signs of GVHD. In this Th1-biased BM environment, host HSCs were observed to persist in the BM, but their maturation was arrested at the ST-HSC stage. This decreased HSC cycling activity was associated with a lack of downstream

progenitor and precursor cells, and ultimately peripheral cytopenias. With resolution of the inflammatory environment (around 4 wk post-HCT), blood formation eventually recovered but continued to be of host origin, indicating failure of donor cells to engraft.

We hypothesize that lack of endogenous HSC division and failure to egress out of the stem cell niche was also a principle reason why donor HSCs failed to engraft. Supplemental Fig. 4 shows our proposed model of the events, which occur after infusion of CD4$^+$-containing grafts into sublethally irradiated hosts. In the presence of minor Ag disparity, interactions between (host) DCs and donor CD4$^+$ T cells elicit reciprocal activation to generate a Th1-type inflammatory environment characterized by IL-12 and IFN-γ. Our results using IFN-γ$^{-/-}$ mice as T cell donors show that alloreactive CD4$^+$ T cells can exert their inhibitory effects on HSC and progenitor cycling activity via this cytokine.

During incidents of stress such as infections, HSC self-renewal and proliferative activity can be triggered by cytokines. Specifically, type I IFNs (IFN-α/β) secreted during viral infections potently stimulate dormant HSCs to proliferate (39, 40). In contrast, IFN-γ, a type II IFN, is classically thought to be an inhibitor of normal hematopoietic progenitor growth of all cell lineages (41, 42). Clinical observations have strongly implicated that overexpression of IFN-γ is a major contributor to the suppression of hematopoiesis in pathogenic BM failure states (22–25). IFN-γ has also been suggested to play a role in the physiologic downregulation
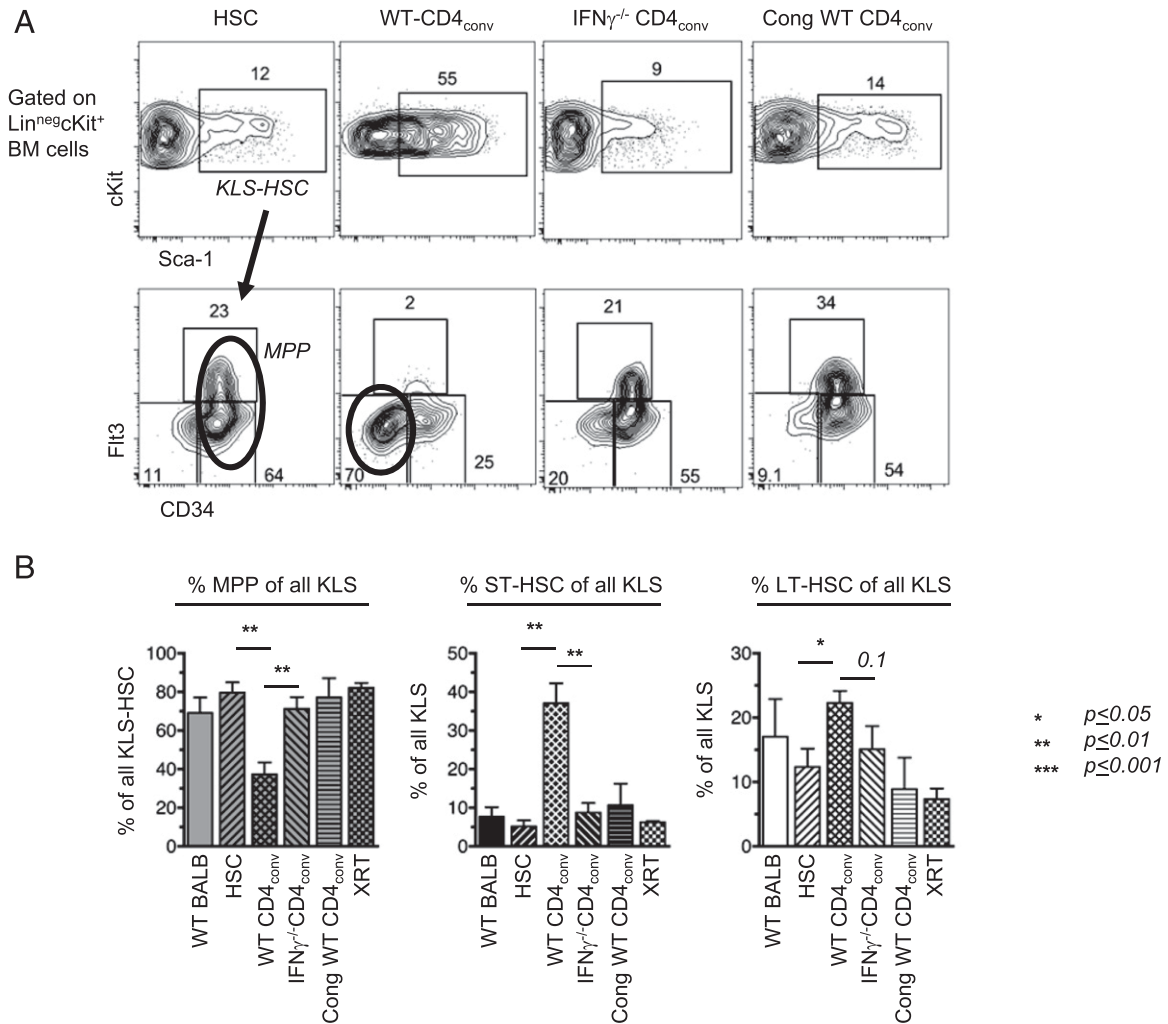
FIGURE 7. CD4-mediated immune injury requires IFN-γ to skew HSC phenotypes. (**A**) Representative FACS plots of BM from sublethally irradiated BALB.B mice on day 14 post-HCT that received 3000 WT HSCs alone ($n = 3$), or HSC+CD4$_{conv}$ taken from WT ($n = 5$) or IFN-γ$^{-/-}$ ($n = 5$) C57BL/6 donors. Control recipients were CD45 congenic C57BL/6 mice that received HSC+WT CD4$_{conv}$ T cells ($n = 2$). BM was analyzed for levels of MPP and true-HSC (ST-HSC and LT-HSC). (**B**) Bar graphs show percent of MPP (left panel), ST-HSC (middle panel), and LT-HSC (right panel) within the KLS-HSC compartment. Compared with all other groups, only recipients of allogeneic HSC+WT CD4$_{conv}$ had a decreased proportion of MPP and increased proportions of ST-HSC and LT-HSC. *$p \leq 0.05$, **$p \leq 0.01$.

of hematopoiesis. Infection of IFN-γ–deficient mice with an avirulent *Mycobacterium bovis* causes development of dramatic and unchecked hyperproliferation of myeloid cells and diminution of lymphocytes, whereas infected WT mice maintain relatively normal leukocyte levels (43). IFN-γ is known to have inhibitory effects on cell cycle progression in a number of different cell types (44–48). De Bruin et al. (49) showed that IFN-γ can act directly on HSCs to reduce their proliferation via deregulation of key cell cycle genes. IFN-γ has also been shown to increase the susceptibility to apoptosis of hematopoietic cells (50).

Despite the literature supporting its negative actions, the effect of IFN-γ on hematopoiesis has recently become a matter of debate. Contrasting the earlier-mentioned studies and our studies are reports that IFN-γ induces the expansion of phenotypic HSCs and/or activates quiescent HSCs to proliferate in the context of certain infections (51, 52). In the latter study by Baldridge et al. (52), IFN-γ produced during infection with *Mycobacterium avium* increased the proliferative fraction of primitive LT-HSCs and resulted in a substantial increase in the number of ST-HSCs. Although our conclusions differ from the latter group, our data are concordant. In this article, we observed a similar proportional

increase in LT-HSCs and ST-HSCs, the early hematopoietic progenitors, in the presence of high marrow IFN-γ; both studies show that in vivo IFN-γ exposure resulted in marked reduction in downstream hematopoietic progenitors and impairment of HSC function. However, our studies diverge in the cell cycling analysis, most likely because of the different settings in which the HSC compartment was interrogated. Baldridge et al. (52) focused on the LT-HSC compartment in the setting of a chronic bacterial infection, whereas we studied cell cycling of the total KLS-HSCs, the majority of which were ST-HSCs, because of the constraints of severe marrow aplasia caused by the allogeneic CD4$^+$ T cells and their graft-versus-host effects on the BM. Thus, it is probable that the context of the exposure of HSCs to IFN-γ, including the degree and length of exposure and other interacting environmental stimuli, will impact on the response of HSCs to this cytokine.

In summary, our studies focused on the activities of conventional allogeneic CD4$^+$ cells on HSC engraftment dynamics. We show that even in the absence of clinically observable GVHD, the BM appears to be highly sensitive to CD4$^+$ cell–mediated Th1 alloreactive responses, which can precipitate a series of interactions leading to marrow aplasia, persistent occupation of

marrow niches by host HSCs, and failure of donor HSCs to engraft. We corroborate the importance of IFN-γ in causing marrow aplasia and further support the role of IFN-γ as a key regulator of hematopoiesis. We show that IFN-γ may exert this regulatory effect by controlling the cycling activity of ST-HSCs. This response of HSCs to environmental conditions induced by CD4$^+$ cell activation brings to light a novel mechanism for failure of HSCs to engraft and has bearing on both clinical transplantation and the understanding of the pathophysiology of BM failure states in general.

Disclosures

The authors have no financial conflicts of interest.

References

1. Lymperi, S., F. Ferraro, and D. T. Scadden. 2010. The HSC niche concept has turned 31. Has our knowledge matured? *Ann. N. Y. Acad. Sci.* 1192: 12–18.
2. Mercier, F. E., C. Ragu, and D. T. Scadden. 2011. The bone marrow at the crossroads of blood and immunity. *Nat. Rev. Immunol.* 12: 49–60.
3. Wilson, A., and A. Trumpp. 2006. Bone-marrow haematopoietic-stem-cell niches. *Nat. Rev. Immunol.* 6: 93–106.
4. Venezia, T. A., A. A. Merchant, C. A. Ramos, N. L. Whitehouse, A. S. Young, C. A. Shaw, and M. A. Goodell. 2004. Molecular signatures of proliferation and quiescence in hematopoietic stem cells. *PLoS Biol.* 2: e301.
5. Wilson, A., E. Laurenti, G. Oser, R. C. van der Wath, W. Blanco-Bose, M. Jaworski, S. Offner, C. F. Dunant, L. Eshkind, E. Bockamp, et al. 2008. Hematopoietic stem cells reversibly switch from dormancy to self-renewal during homeostasis and repair. *Cell* 135: 1118–1129.
6. Cheshier, S. H., S. S. Prohaska, and I. L. Weissman. 2007. The effect of bleeding on hematopoietic stem cell cycling and self-renewal. *Stem Cells Dev.* 16: 707–717.
7. Takizawa, H., R. R. Regoes, C. S. Boddupalli, S. Bonhoeffer, and M. G. Manz. 2011. Dynamic variation in cycling of hematopoietic stem cells in steady state and inflammation. *J. Exp. Med.* 208: 273–284.
8. Baldridge, M. T., K. Y. King, and M. A. Goodell. 2011. Inflammatory signals regulate hematopoietic stem cells. *Trends Immunol.* 32: 57–65.
9. Zhang, P., S. Nelson, G. J. Bagby, R. Siggins, II, J. E. Shellito, and D. A. Welsh. 2008. The lineage-c-Kit+Sca-1+ cell response to *Escherichia coli* bacteremia in Balb/c mice. *Stem Cells* 26: 1778–1786.
10. Massberg, S., P. Schaerli, I. Knezevic-Maramica, M. Köllnberger, N. Tubo, E. A. Moseman, I. V. Huff, T. Junt, A. J. Wagers, I. B. Mazo, and U. H. von Andrian. 2007. Immunosurveillance by hematopoietic progenitor cells trafficking through blood, lymph, and peripheral tissues. *Cell* 131: 994–1008.
11. Nagai, Y., K. P. Garrett, S. Ohta, U. Bahrun, T. Kouro, S. Akira, K. Takatsu, and P. W. Kincade. 2006. Toll-like receptors on hematopoietic progenitor cells stimulate innate immune system replenishment. *Immunity* 24: 801–812.
12. Shimamura, A. 2009. Clinical approach to marrow failure. *Am. Soc. Hematol. Educ. Program* 2009: 329–337.
13. Young, N. S., J. L. Abkowitz, and L. Luzzatto. 2000. New insights into the pathophysiology of acquired cytopenias. *Am. Soc. Hematol. Educ. Program* 2000: 18–38.
14. Young, N. S., R. T. Calado, and P. Scheinberg. 2006. Current concepts in the pathophysiology and treatment of aplastic anemia. *Blood* 108: 2509–2519.
15. Risitano, A. M. 2012. Immunosuppressive therapies in the management of acquired immune-mediated marrow failures. *Curr. Opin. Hematol.* 19: 3–13.
16. Risitano, A. M., J. P. Maciejewski, S. Green, M. Plasilova, W. Zeng, and N. S. Young. 2004. In-vivo dominant immune responses in aplastic anaemia: molecular tracking of putatively pathogenetic T-cell clones by TCR beta-CDR3 sequencing. *Lancet* 364: 355–364.
17. Frickhofen, N., H. Heimpel, J. P. Kaltwasser, and H. Schrezenmeier, German Aplastic Anemia Study Group. 2003. Antithymocyte globulin with or without cyclosporin A: 11-year follow-up of a randomized trial comparing treatments of aplastic anemia. *Blood* 101: 1236–1242.
18. Frickhofen, N., J. P. Kaltwasser, H. Schrezenmeier, A. Raghavachar, H. G. Vogt, F. Herrmann, M. Freund, P. Meusers, A. Salama, and H. Heimpel, The German Aplastic Anemia Study Group. 1991. Treatment of aplastic anemia with antilymphocyte globulin and methylprednisolone with or without cyclosporine. *N. Engl. J. Med.* 324: 1297–1304.
19. Barnes, D. W., and R. H. Mole. 1967. Aplastic anaemia in sublethally irradiated mice given allogeneic lymph node cells. *Br. J. Haematol.* 13: 482–491.
20. Kubota, K., H. Mizoguchi, Y. Miura, S. Kano, and F. Takaku. 1978. Experimental hypoplastic marrow failure in the mouse. *Exp. Hematol.* 6: 791–800.
21. Bloom, M. L., A. G. Wolk, K. L. Simon-Stoos, J. S. Bard, J. Chen, and N. S. Young. 2004. A mouse model of lymphocyte infusion-induced bone marrow failure. *Exp. Hematol.* 32: 1163–1172.
22. Maciejewski, J., C. Selleri, S. Anderson, and N. S. Young. 1995. Fas antigen expression on CD34+ human marrow cells is induced by interferon gamma and tumor necrosis factor alpha and potentiates cytokine-mediated hematopoietic suppression in vitro. *Blood* 85: 3183–3190.
23. Giannakoulas, N. C., M. Karakantza, G. L. Theodorou, M. Pagoni, A. Galanopoulos, T. Kakagianni, A. Kouraklis-Symeonidis, P. Matsouka,

24. A. Maniatis, and N. C. Zoumbos. 2004. Clinical relevance of balance between type 1 and type 2 immune responses of lymphocyte subpopulations in aplastic anaemia patients. *Br. J. Haematol.* 124: 97–105.
24. Sloand, E., S. Kim, J. P. Maciejewski, J. Tisdale, D. Follmann, and N. S. Young. 2002. Intracellular interferon-gamma in circulating and marrow T cells detected by flow cytometry and the response to immunosuppressive therapy in patients with aplastic anemia. *Blood* 100: 1185–1191.
25. Tang, Y., M. J. Desierto, J. Chen, and N. S. Young. 2010. The role of the Th1 transcription factor T-bet in a mouse model of immune-mediated bone-marrow failure. *Blood* 115: 541–548.
26. Maciejewski, J. P., C. Selleri, T. Sato, S. Anderson, and N. S. Young. 1996. A severe and consistent deficit in marrow and circulating primitive hematopoietic cells (long-term culture-initiating cells) in acquired aplastic anemia. *Blood* 88: 1983–1991.
27. Martin, P. J., Y. Akatsuka, M. Hahne, and G. Sale. 1998. Involvement of donor T-cell cytotoxic effector mechanisms in preventing allogeneic marrow graft rejection. *Blood* 92: 2177–2181.
28. Kernan, N. A., C. Bordignon, G. Heller, I. Cunningham, H. Castro-Malaspina, B. Shank, N. Flomenberg, J. Burns, S. Y. Yang, P. Black, et al. 1989. Graft failure after T-cell-depleted human leukocyte antigen identical marrow transplants for leukemia: I. Analysis of risk factors and results of secondary transplants. *Blood* 74: 2227–2236.
29. Marmont, A. M., M. M. Horowitz, R. P. Gale, K. Sobocinski, R. C. Ash, D. W. van Bekkum, R. E. Champlin, K. A. Dicke, J. M. Goldman, R. A. Good, et al. 1991. T-cell depletion of HLA-identical transplants in leukemia. *Blood* 78: 2120–2130.
30. Martin, P. J., J. A. Hansen, B. Torok-Storb, D. Durnam, D. Przepiorka, J. O'Quigley, J. Sanders, K. M. Sullivan, R. P. Witherspoon, H. J. Deeg, et al. 1988. Graft failure in patients receiving T cell-depleted HLA-identical allogeneic marrow transplants. *Bone Marrow Transplant.* 3: 445–456.
31. Jakubowski, A. A., T. N. Small, J. W. Young, N. A. Kernan, H. Castro-Malaspina, K. C. Hsu, M. A. Perales, N. Collins, C. Cisek, M. Chiu, et al. 2007. T cell depleted stem-cell transplantation for adults with hematologic malignancies: sustained engraftment of HLA-matched related donor grafts without the use of antithymocyte globulin. *Blood* 110: 4552–4559.
32. Martin, P. J. 1993. Donor CD8 cells prevent allogeneic marrow graft rejection in mice: potential implications for marrow transplantation in humans. *J. Exp. Med.* 178: 703–712.
33. Palathumpat, V., S. Dejbakhsh-Jones, and S. Strober. 1995. The role of purified CD8+ T cells in graft-versus-leukemia activity and engraftment after allogeneic bone marrow transplantation. *Transplantation* 60: 355–361.
34. Jiang, Z., G. B. Adams, A. M. Hanash, D. T. Scadden, and R. B. Levy. 2002. The contribution of cytotoxic and noncytotoxic function by donor T-cells that support engraftment after allogeneic bone marrow transplantation. *Biol. Blood Marrow Transplant.* 8: 588–596.
35. Feinstein, L., B. Sandmaier, D. Maloney, P. A. McSweeney, M. Maris, C. Flowers, J. Radich, M. T. Little, R. A. Nash, T. Chauncey, et al. 2001. Nonmyeloablative hematopoietic cell transplantation. Replacing high-dose cytotoxic therapy by the graft-versus-tumor effect. *Ann. N. Y. Acad. Sci.* 938: 328–337; discussion 337–329.
36. Gyurkocza, B., R. Storb, B. E. Storer, T. R. Chauncey, T. Lange, J. A. Shizuru, A. A. Langston, M. A. Pulsipher, C. N. Bredeson, R. T. Maziarz, et al. 2010. Nonmyeloablative allogeneic hematopoietic cell transplantation in patients with acute myeloid leukemia. *J. Clin. Oncol.* 28: 2859–2867.
37. Müller, A. M., J. A. Linderman, M. Florek, D. Miklos, and J. A. Shizuru. 2010. Allogeneic T cells impair engraftment and hematopoiesis after stem cell transplantation. *Proc. Natl. Acad. Sci. USA* 107: 14721–14726.
38. Müller, A. M., S. Shashidhar, N. J. Küpper, H. E. Kohrt, M. Florek, R. S. Negrin, J. M. Brown, and J. A. Shizuru. 2012. Co-transplantation of pure blood stem cells with antigen-specific but not bulk T cells augments functional immunity. *Proc. Natl. Acad. Sci. USA* 109: 5820–5825.
39. Essers, M. A., S. Offner, W. E. Blanco-Bose, Z. Waibler, U. Kalinke, M. A. Duchosal, and A. Trumpp. 2009. IFNalpha activates dormant haematopoietic stem cells in vivo. *Nature* 458: 904–908.
40. Sato, T., N. Onai, H. Yoshihara, F. Arai, T. Suda, and T. Ohteki. 2009. Interferon regulatory factor-2 protects quiescent hematopoietic stem cells from type I interferon-dependent exhaustion. *Nat. Med.* 15: 696–700.
41. Selleri, C., T. Sato, S. Anderson, N. S. Young, and J. P. Maciejewski. 1995. Interferon-gamma and tumor necrosis factor-alpha suppress both early and late stages of hematopoiesis and induce programmed cell death. *J. Cell. Physiol.* 165: 538–546.
42. Yu, J. M., R. V. Emmons, Y. Hanazono, S. Sellers, N. S. Young, and C. E. Dunbar. 1999. Expression of interferon-gamma by stromal cells inhibits murine long-term repopulating hematopoietic stem cell activity. *Exp. Hematol.* 27: 895–903.
43. Murray, P. J., R. A. Young, and G. Q. Daley. 1998. Hematopoietic remodeling in interferon-gamma-deficient mice infected with mycobacteria. *Blood* 91: 2914–2924.
44. Arens, R., K. Tesselaar, P. A. Baars, G. M. van Schijndel, J. Hendriks, S. T. Pals, P. Krimpenfort, J. Borst, M. H. van Oers, and R. A. van Lier. 2001. Constitutive CD27/CD70 interaction induces expansion of effector-type T cells and results in IFNgamma-mediated B cell depletion. *Immunity* 15: 801–812.
45. de Bruin, A. M., M. Buitenhuis, K. F. van der Sluijs, K. P. van Gisbergen, L. Boon, and M. A. Nolte. 2010. Eosinophil differentiation in the bone marrow is inhibited by T cell-derived IFN-gamma. *Blood* 116: 2559–2569.

46. de Bruin, A. M., S. F. Libregts, M. Valkhof, L. Boon, I. P. Touw, and M. A. Nolte. 2012. IFNγ induces monopoiesis and inhibits neutrophil development during inflammation. *Blood* 119: 1543–1554.

47. Libregts, S. F., L. Gutiérrez, A. M. de Bruin, F. M. Wensveen, P. Papadopoulos, W. van Ijcken, Z. Ozgür, S. Philipsen, and M. A. Nolte. 2011. Chronic IFN-γ production in mice induces anemia by reducing erythrocyte life span and inhibiting erythropoiesis through an IRF-1/PU.1 axis. *Blood* 118: 2578–2588.

48. Young, H. A., D. M. Klinman, D. A. Reynolds, K. J. Grzegorzewski, A. Nii, J. M. Ward, R. T. Winkler-Pickett, J. R. Ortaldo, J. J. Kenny, and K. L. Komschlies. 1997. Bone marrow and thymus expression of interferon-gamma results in severe B-cell lineage reduction, T-cell lineage alterations, and hematopoietic progenitor deficiencies. *Blood* 89: 583–595.

49. de Bruin, A. M., Ö. Demirel, B. Hooibrink, C. H. Brandts, and M. A. Nolte. 2013. Interferon-γ impairs proliferation of hematopoietic stem cells in mice. *Blood* 121: 3578–3585.

50. Rathbun, R. K., G. R. Faulkner, M. H. Ostroski, T. A. Christianson, G. Hughes, G. Jones, R. Cahn, R. Maziarz, G. Royle, W. Keeble, et al. 1997. Inactivation of the Fanconi anemia group C gene augments interferon-gamma-induced apoptotic responses in hematopoietic cells. *Blood* 90: 974–985.

51. Zhao, X., G. Ren, L. Liang, P. Z. Ai, B. Zheng, J. A. Tischfield, Y. Shi, and C. Shao. 2010. Brief report: interferon-gamma induces expansion of Lin(-)Sca-1(+)C-Kit(+) Cells. *Stem Cells* 28: 122–126.

52. Baldridge, M. T., K. Y. King, N. C. Boles, D. C. Weksberg, and M. A. Goodell. 2010. Quiescent haematopoietic stem cells are activated by IFN-gamma in response to chronic infection. *Nature* 465: 793–797.